vapor through the gas at the test temperature and the pressure $P_\infty$, $m^2/sec$; η, viscosity of vapor–gas mixture averaged over the partial pressures [3], $N \cdot sec/m^2$; M, mass density of the vapor flow, $kg/m^2 \cdot sec$; $R = R_0/\mu$, specific gas constant, J/kg•K; μ, molecular weight of liquid being evaporated, kg/kmole; T, temperature, °K; $l$, coordinate of meniscus of liquid during evaporation, m; ρ, density of liquid, $kg/m^3$; t, time, sec; $R_0$, universal gas constant.

## LITERATURE CITED


1. G. F. Ershova, Z. M. Zorin, and N. V. Churaev, "Temperature dependence of the thickness of polymolecular adsorption films of water on a quartz surface," Kolloidn. Zh., No. 1, 208-210 (1975).
2. P. D. Lebedev, Drying with Infrared Radiation [in Russian], Gosénergoizdat, Moscow–Leningrad (1955).
3. M. N. Gaidukov, N. V. Churaev, and Yu. I. Yalamov, "Theory of evaporation of liquids from capillary tubes at a temperature above the boiling point," Zh. Tekh. Fiz., No. 10, 2142-2147 (1976).
4. N. B. Vargaftik, Handbook of Thermophysical Properties of Gases and Liquids [in Russian], Nauka, Moscow (1972).
5. M. P. Vukalovich, S. L. Rivkin, and A. A. Aleksandrov, Tables of Thermophysical Properties of Water and Water Vapor [in Russian], Standartov, Moscow (1969).
6. S. N. Zotov, Ya. I. Rabinovich, and N. V. Churaev, "Experimental study of the high-temperature evaporation of liquids from capillary tubes," Inzh.-Fiz. Zh., No. 6, 1035-1039 (1978).


# EXPERIMENTAL INVESTIGATION OF THE WORKING PROCESS IN A VORTEX TUBE

V. A. Vysochin and V. A. Safonov

UDC 532.527

The authors present the results of an experimental investigation of the temperature separation process in the chamber of an energy separation vortex tube.

The use of the vortex effect in industry requires improvement both in vortex tubes themselves and in the method of their design. This can be achieved primarily by the accumulation of information on the nature of the processes occurring in a vortex tube. Unfortunately, the experimental study of the high-speed three-dimensional flow in small diameter vortex tubes is very complex, and the published data are few and have not been classified. In this paper, besides the experimental investigation, the authors have tried to analyze flow within the energy separation chamber of a vortex tube.

The tests were performed in a counterflow adiabatic vortex tube with a cylindrical energy separation chamber of diameter 0.1 m. A four-channel nozzle insert was made up in the form of an Archimedes spiral with a total geometrical area of channels of 0.1 F at the throat section. The relative diameter of the diaphragm aperture was $\bar{d} = 0.5$. The relative roughness of the inner surface of the energy separation chamber was $\bar{\Delta} = 1 \cdot 10^{-3}$. The chamber length was 12.5D.

The flow parameters inside the energy chamber were investigated at four sections. Section I was at a distance of 0.01 m ($\bar{L} = 0.1$) from the diaphragm plane, and sections II, III, and IV were at distances of $\bar{L} = 1.5$, 5.0 and 8.5, respectively.

To investigate the distribution of the parameters at sections II-IV we used a variable-attitude combination Γ-shaped head, made of a tube of outer diameter 0.001 m according to the recommendations of [1]. Before the investigations were conducted the head was calibrated in a wind tunnel in the test range of reduced flow velocities.

The radial distribution of stagnation temperature and pressure at the nozzle section ($\bar{L} = 0.1$) was investigated by means of two heads which were inserted into the vortex tube

N. É. Zhukovskii Order of Lenin Kharkov Aviation Institute. Translated from Inzhenerno-Fizicheskii Zhurnal, Vol. 44, No. 2, pp. 235-242, February, 1983. Original article submitted August 24, 1981.

  

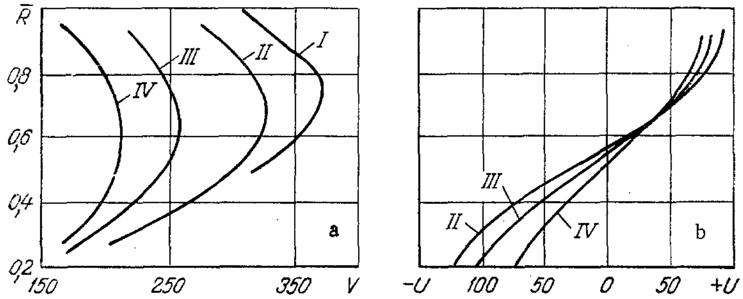

Fig. 1. Radial graphs of the circumferential (a) and axial (b) velocities in the energy chamber of a vortex tube: I) $\bar{L}$ = 0.1; II) 1.5; III) 5.0; IV) 8.5. V and U are in m/sec.

through apertures in the diaphragm. The static pressures at these sections were measured by means of 15 taps located along the radius of the diaphragm. Experiments showed that this method of obtaining information at section I made it possible to minimize the error in measuring static pressures and eliminated distortion of the flow picture due to the head support. To measure the flow temperature at section I we used a head made of type KTMS (Chromel—Copel) thermocouple cable with an envelope diameter of 0.0015 m. The thermocouple junction had a diameter of 0.0005 m. The sensor part of the stagnation pressure head, made of a tube of outer diameter 0.001 m, had a chamber to ensure that it was insensitive to flow angle in the range ±23°. As secondary instruments to record the temperatures and pressures, we used type GRM-2 group recording manometers and type KSP-4 electronic potentiometers.

The investigations were conducted in air with the inlet conditions: $T^* = 373 \pm 2°K$, $p^* \leqslant 6 \cdot 10^5$ N/m$^2$ ($\pi^* \leqslant 6.0$). The values of $\mu$ were determined by calculation, for which purpose we measured the flow rates of air arriving at the nozzle insert and of the heated flow.

The circumferential and axial components of the flow velocity were calculated at various sections from the measured flow angles, reduced velocities, and stagnation temperatures. To determine the stagnation temperatures we calculated the recovery factor of a specific thermocouple as recommended in [1].

Reduction of the experimental data showed that, as the swirling flow moved along the energy separation chamber of the vortex tube, its circumferential velocity component reduced (Fig. 1a), and this was seen more intensely in the peripheral part. Here the axial velocity gradients reach values of 6-7% over the diameter. Comparison of the circumferential velocity graphs over a wide range of $\mu$ shows that in the hot part there is apparently no appreciable redistribution of the radial graph of the circumferential velocities along the length. Basically the flow retains a single complex type of vortex from section I to section IV, described in general by the equation $VR^n$ = const, with a maximum velocity reaching $\bar{R} \approx 0.75$ at section I and $\bar{R} \approx 0.60$ at section IV. Analysis of the radial graphs of axial velocities in Fig. 1b shows that the flow in the peripheral part of the energy separation chamber is accompanied by a decrease of the flow rate of the component of absolute velocity from the nozzle section to the valve section, while in the near-axial part it increases from the valve section to the nozzle. The radius of the conventional interface between the peripheral and axial regions in our experiment is close to the radius of the diaphragm aperture and depends slightly on $\bar{L}$ and $\mu$.

As a whole, the velocity distribution obtained confirms the known picture of two-dimensional flow [2]. The radial velocity component can be obtained by calculation.

Having available data on the distribution of pressure, temperature, and flow angle along the radius, we can calculate the axial mass flux along the energy chamber of the vortex tube. The calculations were carried out by numerical integration of the flow rate over the cross section from the radius of the conventional interface of the two flows (U = 0) up to the generators of the energy chamber for the peripheral flow. For the axial flux the integration was carried out in the range $(R_1 = 0) \leqslant R \leqslant (R_2 = R_{U=0})$. Figure 2a shows the results of calculations of the ratio of the mass of flux for the peripheral region to the mass of gas arriving through the nozzle insert. In the region of $\mu$ investigated the experimental curves can be approximated by the equation

$$\bar{m} = \exp(-0.124\mu\bar{L}). \quad (1)$$

It can be seen from Fig. 2a that the displacement of the gas stream from the nozzle section to the throttle valve is accompanied by a reduction in mass in the peripheral region, and with

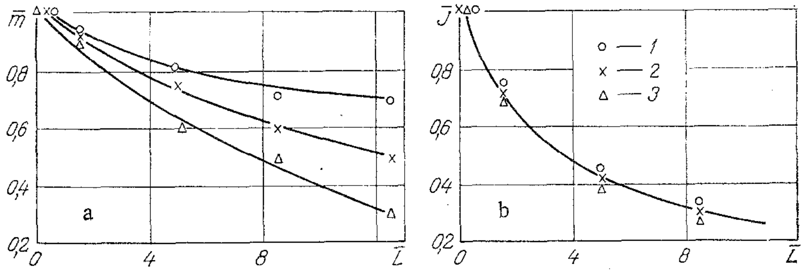


Fig. 2. Variation in the flow of mass (a) and momentum (b) along the energy chamber of a vortex tube: 1) $\mu$ = 0.3; 2) 0.5; 3) 0.7.

the greatest gradients in the initial sections. For a total length of energy chamber of $\overline{L}$ = 12.5, apart from the dependence on $\mu$, 33% of the reduction of mass flux in the peripheral region occurs in the section of ~3.0 diameters, and 50% of the reduction occurs within a section of extent 4.6 diameters. The decrease of mass in the peripheral section evidently results from leakage into the axial region, due to the presence of a radial velocity component.

The radial velocity, referenced to the parameters of the gas stream at the conventional interface, can be calculated from the mass equation. It turns out that the maximum values of radial velocities also correspond to the initial sections, but they are very small in absolute value. For instance, for the initial sections W did not exceed a value of 0.006 $V_{max}$ for these sections. Up to the fourth section W under the same conditions ($\mu$ = 0.7) decreased monotonically to 0.004 $V_{max}$. The smallness of the radial velocities can be explained by the considerable values of surface sink. Here the radial velocities were calculated as mass flow averages.

From the available experimental data one can analyze the variation of momentum flux in the peripheral region of the energy chamber. The results of the calculations are shown in Fig. 2b. The momentum flux is referenced to the flow parameters at the exit of the nozzle insert. It follows from the graph that the variation in reduced momentum along the energy chamber is also exponential and can be expressed in the form

$$\overline{J} = \exp(-0.18\overline{L}). \qquad (2)$$

The presence of an axial momentum flux gradient, in conjunction with a radial efflux of working substance, allows an analogy to be drawn between the process of expanding a gas in the energy separation chamber of a vortex tube and the peculiar turbine friction in which a reduction of the gas stagnation temperature results from its doing work [3]. With this analogy one can design vortex tubes without resorting to the complex model of the energy exchange process suggested in [2].

We shall now analyze graphs of the radial distribution of the flow parameters at the nozzle section at relative flow rates of cold flow of $\mu$ = 0.5 (Fig. 3a). At the exit from the channels of the nozzle insert the flow has a subsonic velocity averaged around the circumference. As the radius decreases from $\overline{R}$ = 1.00 to $\overline{R}$ = 0.80, the flow accelerates up to sonic and supersonic velocities according to a law that is described very closely by the free vortex equation VR = const. At this same section the stagnation pressure is kept constant along the radius. Starting from $\overline{R} \approx 0.80$ there is a transition section where the radial variation of velocity is described by the equation $VR^n$ = const. At this section the exponent of R changes from n = +1 to n = −1, i.e., the flow acceleration continues with subsequent deceleration and transition through sonic velocity. The reduction of stagnation temperature begins with $\overline{R} \approx$ 0.80 (for $\mu$ = 0.3 $\overline{R}$ = 0.85; $\mu$ = 0.7 $\overline{R}$ = 0.63).

As is known from hydromechanics, a dependence of the form VR = const is called a potential vortex, the law of constant circulation, and constancy of angular momentum. In accordance with this law the stagnation pressure and the stagnation temperature stay constant in the region where this type of vortex exists. In other words, the flow acceleration in this section occurs in the same way as for the bladeless directional apparatus of a centripetal turbine [4].

Analysis of the ratios of the measured flow parameters in the range $\overline{R}$ = 0.80-0.50 shows that in this section a decrease of the stagnation pressure is equivalent to a decrease of

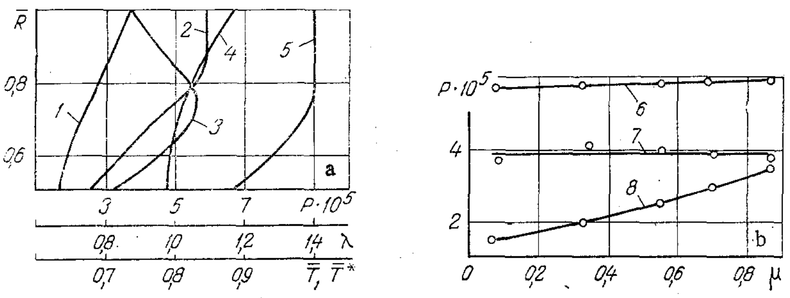


Fig. 3. Distribution of parameters at the nozzle insert section of the vortex tube: 1) p; 2) $p^*$; 3) λ; 4) $\bar{T}$; 5) $\bar{T}^*$; 6) $p_1^*$; 7) $p_{1meas}^*$; 8) $p_2^*$. p is in $N/m^2$.

stagnation temperature and to the dissipative losses. The decrease of stagnation pressure in an ideal process equivalent to the stagnation temperature decrease can be found from the isentropic equation

$$T_2^*/T_1^* = (p_2^*/p_1^*)^{k-1/k}. \tag{3}$$

The difference $p_1^* - p_{1meas}^*$ is the dissipative losses. Figure 3b shows the results of the calculations using Eq. (3) in the range of μ investigated. It can be seen from Fig. 3b that the dissipative losses of stagnation pressure linked to the vortex character of the flow depend slightly on μ, and (for a given degree of expansion) can be taken to be roughly equal to $0.34p_1^*$. The relative loss, expressed in terms of the efficiency of the expansion process, can be calculated from the equation

$$T_1^* - T_2^* = \eta^* T_1^* [1-(p_2^*/p_1^*)^{k-1/k}]. \tag{4}$$

The results of the efficiency calculations from the stagnation parameters for four sections of the energy chamber of the vortex tube for different values of μ are shown in Table 1, from which it can be seen that the relative losses increase monotonically with increase of the relative mass flow rate of cooled gas. The losses also increase with increasing distance from the nozzle insert section, going towards the throttle valve. At the same time, the fact that the values of $\eta^*$ at different sections along the energy chamber are commensurate with the temperature coefficient of the vortex tube efficiency η is evidence that the processes occurring are common.

Analysis of the T = f(R) curve shows that the minimum of the static temperature in the range of the experiment performed at the nozzle insert section occurs at $\bar{R}$ = 0.50–0.80, depends on μ, and is governed, apparently, by the set of velocities and ambient stagnation temperatures at a given radius. The radial gradients of the measured static pressures are found to be in accordance with the equilibrium equation for swirling flow.

From the available experimental data one can calculate the drag coefficient for flow of the peripheral stream from the nozzle insert section to the throttle valve and the loss coefficients for flow of gas in the radial direction. This kind of differentiated approach to determining the hydraulic loss coefficients is desirable to resolve the matter of the limit characteristics of the vortex tube.

The hydraulic drag coefficients of the peripheral flow were calculated from the formula

$$\zeta = \frac{2\Delta p^*}{\rho C^2} \frac{\cos(\widehat{CU})}{\bar{L}}, \tag{5}$$

and the Re number:

$$\mathrm{Re} = CD/\nu. \tag{6}$$

The values of $\Delta P^*$ in Eq. (5) were determined in the range between the measuring sections at the reduced radius $\bar{R}$ = 0.90, corresponding to the "core" of the stagnation pressure curve. The remaining values appearing in Eqs. (5) and (6) correspond to average parameters of the gas stream at the same $\bar{R}$ in the given range $\bar{L}$. As the characteristic dimension in Eq. (6), we took the vortex tube energy chamber diameter. The results of the calculations according to Eqs. (5) and (6) are given in Table 2 from which it can be seen that the flow in the peripheral part of the energy chamber corresponds to the similarity solution for the Reynolds number region, and a change of Reynolds number from Re = $1.86\cdot10^6$ to Re = $4.87\cdot10^6$ has

TABLE 1. Distribution of the Efficiency of the Expansion Process $\eta^*$ at Various Sections of the Vortex Tube as a Function of $\mu$

| $\mu$ | $\bar{L}$ | | | | |
|---|---|---|---|---|---|
| | 0,1 | 1,5 | 5,0 | 8,5 | $\eta$ |
| 0,3 | 69,6 | 66,2 | 57,5 | 52,0 | 54,6 |
| 0,5 | 60,4 | 54,7 | 45,5 | 39,5 | 47,3 |
| 0,7 | 45,7 | 39,5 | 31,4 | 27,5 | 32,7 |

TABLE 2. Calculated Hydraulic Loss Coefficient along the Vortex Tube Energy Separation Chamber

| $\mu$ | 0,3 | | | 0,5 | | | 0,7 | | |
|---|---|---|---|---|---|---|---|---|---|
| $N_{\text{section}}$ | I—II | II—III | III—IV | I—II | II—III | III—IV | I—II | II—III | II—IV |
| $\zeta$ | 0,097 | 0,096 | 0,096 | 0,089 | 0,094 | 0,094 | 0,095 | 0,091 | 0,096 |
| $\text{Re}\cdot 10^{-6}$ | 4,87 | 3,22 | 2,17 | 4,86 | 3,20 | 2,00 | 4,63 | 2,84 | 1,86 |

practically no influence on the hydraulic drag coefficient $\zeta$. The absolute value of the hydraulic drag coefficient is interesting. It is almost five times larger than the drag coefficient in flow without twist in steel pipes of analogous roughness [5]. The probable reason for this, in addition to the specific features of swirling flow [6], is the efflux of working substance from the peripheral region towards the axis. Tests with porous tubes [7] have shown that this factor has a very important influence on the hydraulic loss.

According to [8], for the strongly swirling flows which are observed in cyclone-vortex chambers and vortex tubes, the tangential friction stresses for the main part of the flow can be represented in the form

$$\tau = \mathrm{K}\rho\,(d\Gamma/dR)^2, \tag{7}$$

where K is a parameter describing the turbulent structure of the flow; and $\Gamma = VR$ is the velocity circulation.

Analysis of the curves of T* and $p^* = f(\bar{R})$ has shown that the hydraulic losses of stagnation pressure in the radial direction are proportional to the friction stresses and can be calculated from the formula

$$\Delta p^* = \frac{\Delta R}{R_{\text{av}}}\,\mathrm{K}\rho_{\text{av}}(\Delta\Gamma/\Delta R)^2. \tag{8}$$

It follows from Eqs. (7) and (8) that for circulation-free flow ($\Gamma = VR = \text{const}$) the friction stresses and the stagnation pressure losses in the radial direction are zero. This finds an experimental confirmation at the nozzle insert section at the segment $0.80 \leqslant \bar{R} \leqslant 1.00$ (Fig. 3a).

The reduction of the radial curves of p* and $T^* = f(R)$ has shown that there is quite a close connection between the dimensionless quantities K and $R_v/R_{v\max}$. An empirical relation (with correlation coefficient r = 0.91) can be represented in the form of the expression

$$\mathrm{K} = 0.5\,(R_v/R_{v\,\max})^{3.2} \tag{9}$$

for the range $0.1 \leqslant \bar{L} \leqslant 1.5$ and $\mu = 0.12\text{–}0.50$.

From the experimental data obtained and the calculated hydraulic loss coefficients we can improve the flow structure in large-scale vortex tubes and plan ways to perfect them.

## NOTATION

D, F, diameter and area of the energy separation chamber at the nozzle insert section; $\bar{d}$, relative diameter of the diaphragm aperture; $\bar{L}$, reduced length of the energy separation chamber; m, mass flow rate; p, p*, static pressure, stagnation pressure: T', T, T*, measured, static and stagnation temperature; $\bar{T}$, $\bar{T}^*$, static and stagnation temperature referenced to the stagnation temperature at the nozzle exit; R, $\bar{R}$, ambient and reduced radii; r, thermocouple recovery factor, or correlation coefficient; Re, Reynolds number; C, V, U, W, absolute, circumferential, axial, and radial velocity components; $\zeta$, hydraulic drag coefficient; $\eta = \Delta T^*/$

$\Delta T_S^*$, coefficient of thermal efficiency; $\lambda$, velocity coefficient; $\mu = m_\chi/m_0$, relative mass flow rate of cold stream; $\rho$, density. Subscripts: 1, 2, 0, x, for the parameters of the beginning and end of the expansion process for cold flow arriving at the nozzle insert.

## LITERATURE CITED


1. N. F. Peshekhonov, Instruments to Measure the Pressure, Temperature, and the Direction of Flow in Compressors [in Russian], Oborongiz, Moscow (1962).
2. A. P. Merkulov, The Vortex Effect and Its Application in Technology [in Russian], Mashinostroenie, Moscow (1969).
3. I. A. Charnyi, "Theory of the vortex cooler," Izv. Akad. Nauk SSSR, Otd. Tekh. Nauk, No. 6, 148 (1962).
4. V. T. Mitrokhin, Choice of Parameters and Design of the Centripetal Turbine for Steady and Transitional Conditions [in Russian], Mashinostroenie, Moscow (1974).
5. M. E. Deich, Engineering Gasdynamics [in Russian], Gosénergoizdat, Moscow—Leningrad (1961).
6. V. K. Shchukin, Heat Transfer and Hydrodynamics of Internal Flows in Mass Force Fields [in Russian], Mashinostroenie, Moscow (1970).
7. V. S. Mikhailov et al., "Experimental investigation of the flow momentum and friction coefficients with uniform efflux in a porous tube," Inzh.-Fiz. Zh., 30, No. 6, 1003 (1976).
8. A. N. Shtym, "Determination of the tangential friction stress in a rotating stream of gas," in: Some Topics in the Investigation of the Vortex Effect and Its Industrial Application [in Russian], Kuibyshev Aviation Inst. (1974).


# NONEQUILIBRIUM NEGATIVE PRESSURES


F. G. Veliev



UDC 532.552



The possibility of obtaining brief negative pressures in real pipeline systems under definite nonequilibrium processes is experimentally considered.


A negative pressure is one of the metastable states at which the effect of tension and the subsequent discontinuity of the fluid appears. There are numerous results of experimental researches of static and dynamic nature in which a negative pressure appears to some degree [1]. Starting with the first tests of F. M. Donny, who obtained a negative pressure of just −0.12 bar and ending with the researches of L. J. Briggs who reached the value −425 bar, the main condition for the appearance of the effect in the tests performed was adequate "purity" of the fluid and the vessel, i.e., absence of any gas bubbles, impurities, foreign films, etc.

We investigated the condition for the origination of negative pressures in real pipeline systems for definite nonequilibrium transients. The diagram of the experimental set-up is represented in Fig. 1, where 1 is the high-pressure trap (3 $m^3$); 2 is the pipeline; 3 is the shutoff valve; 4 is a chromel-kopel thermocouple; 5 is a differential manometer; 6 is a valve; 7 is a tank; 8 are regulating gates; 9 are pumps; D are pressure strain gauges; DV is a Dewar vessel; P is the potentiometer P-363/1; CP is the control panel; Osc is the oscilloscope K12-22; A is an amplifier, and PR is a pressure regulation system. The working length of the horizontally mounted steel pipeline was 30 m. The cutoff valve assured practically instantaneous ($10^{-2}$ sec) turn-on (or off) of the flow. The characteristic of the nonstationary process originating in the flow was recorded by the oscilloscope and potentiometer by means of appropriate pressure and temperature sensors. Semiconductor strain gauges developed in the Institute of Physics of the Academy of Sciences of the Azerbijan SSR were used as pressure sensors [2].

Water and viscoelastic oil from the Balakhyn—Sabunchi—Romaninskii deposits were used in the tests. When the cutoff valve was opened the fluid under investigation flowed into the


M. Azizbekov Azerbaidzhan Institute of Oil and Chemistry, Baku.


Translated from Inzhenerno-Fizicheskii Zhurnal, Vol. 44, No. 2, pp. 242-244, February, 1983. Original article submitted January 11, 1982.




0022-0841/83/4402-0164$07.50